COMPARING THE MORPHOLOGY OF LONGITUDINAL STRIATIONS ON MARTIAN LANDSLIDE DEPOSITS AND EJECTA BLANKETS. A. Pietrek[1], S. Hergarten[1] and T. Kenkmann[1], [1]Institute of Earth and Environmental Sciences - Geology, Albert-Ludwigs-University Freiburg, Germany (alexa.pietrek@geologie.uni-freiburg.de).

Introduction: Distinct longitudinal grooves and ridges ("striations") are an enigmatic and unexplained feature of long run-out landslides on Earth [1,2,3] and Mars [4,5,6,7]. They form in different materials and in a wide variety of geological settings, for example in rock avalanches [3,13,15], landslides deposited on a glacial substrate [1] and volcanic debris flows [2,15]. Similar features can also be observed on the ejecta blankets of Martian SLE (single-layered ejecta) craters and DLE (double-layered ejecta) craters [6,9,10,12]. Several formation mechanisms have been proposed [11,12,13,6,8,9,10], but it remains a central question whether the striations on different types of deposits form by a common mechanism. We conducted a morphometric analysis on topographic profiles of well-preserved Martian landslides and ejecta blankets of DLE and SLE craters to evaluate the possibility of common formation processes.

Methods: The analysis was conducted for the landslides Coprates Labes (11°54' S, 67°45' W), Ophir Labes (11°01' S, 67°59' W), Melas Labes (8°55' S, 71°53' W), two unnamed landslides situated in Capri Chasma (*Capri1*: 8°37' S, 44°33' W; *Capri2*: 7°37' S, 44°12' W), an unnamed landslide deposited in Blunck crater (BL: 27°32' S, 37°02' W), the DLE craters Steinheim (54°34' N, 169°22' W) and Bacolor (32°57' N, 118°37' E) and an unnamed SLE crater (*SL5*, 34°13' N, 109°35' E).

CTX and HiRISE data for all datasets were processed with the ISIS software. DEMs from CTX and HiRISE stereo pairs were processed with the AMES stereo pipeline [14]. Profiles were extracted with a sampling distance of 10 m in longitudinal and perpendicular direction relative to the striations. The perpendicular profiles have an equal spacing of 0.5 km. For comparison, randomly oriented profiles were extracted from the surrounding terrain as well. We presume that the topography of the surrounding terrain approximates the substrate topography prior to the emplacement of our deposits. We conducted a Fourier analysis of the topography tracks and visualized the results as power spectrums. The power law dependence of the power spectral density on wavenumber was fitted using a Maximum Likelihood Method. The fit has the form $S(f) = \gamma + \alpha f^{-\beta}$, where *S(f)* is the power spectral density, *f* is wavenumber, γ is noise, α is a scaling factor and β the power law exponent.

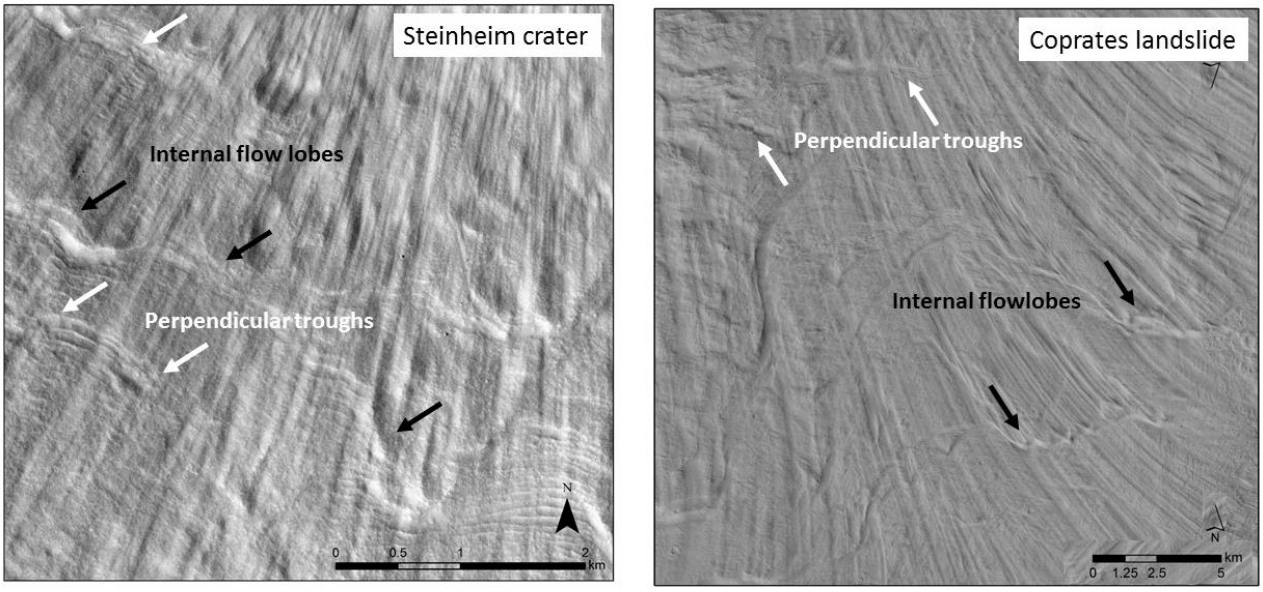

Figure 1: Striations on ejecta blankets (left) and landslide deposits (right) share a number of morphological features: internal flow lobes (white arrows), perpendicular troughs (black arrows) and perpendicular compressive ridges (southwest corner of left image) can be found on almost all of the deposits. Perpendicular troughs and ridges typically overprint striations, which implies that those structures formed later.

Results and Discussion: The power spectral densities of the topographies all have a power law dependency on frequency, which indicates that the topography of the striations is scale-invariant (Fig. 2). This inherently means that striations have strongly varying widths: there is no equal spacing and no "typical" width that could be used to characterize the deposits. A power law relationship with β=2 is also known as Brownian motion and also reported for topography [15]. The exponent β can be interpreted as surface roughness. A higher exponent signifies a higher content of low frequencies in the topographic signal. In the spatial domain, this translates to a greater importance of long wavelengths. Therefore higher values describe a smoother surface.

Several relationships can be concluded from a preliminary summary of results:

A) We found that the power law exponents cover a wide range of values between β=1.5 and β=3.5 (Fig. 2). Most of the profiles have a value significantly greater than the expected value of 2. Although the overall range is large, each deposit only has a specific, limited range of values.

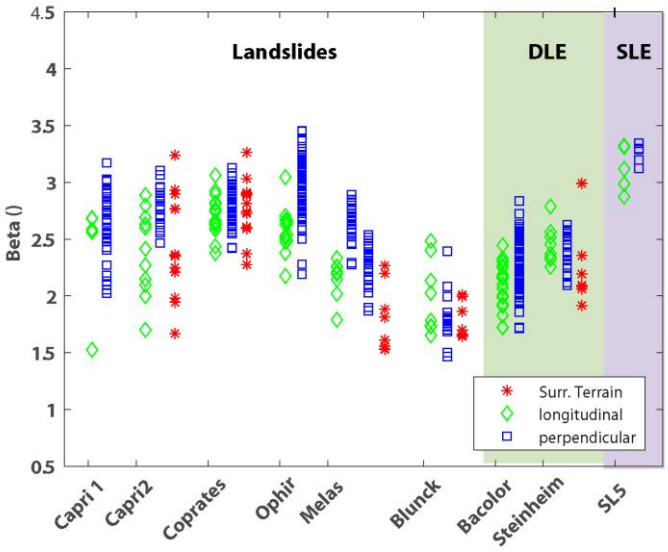

Figure 2: Summary plot of the power law exponents β for perpendicular and longitudinal profiles across striations and profiles from the surrounding terrain. For all deposits, the exponents for longitudinal and perpendicular topography tracks are within a close range and in turn are very similar to the exponents of the surrounding terrain.
Note: At the current state, terrain data was not available for some datasets. The terrain data for both Capri landslides was extracted in the area between both deposits. For Melas Labes, perpendicular profiles were extracted in two different locations.

B) The comparison between longitudinal and perpendicular profiles shows that the power law exponents are within a similar range for each deposit. A closer inspection of the profiles reveals that the profiles in perpendicular direction have a stronger relief. This is consistent with a horizontal scaling of the topography in perpendicular direction with respect to the topography in longitudinal direction.

C) The power law exponents for the profiles of the surrounding terrain are very close in range to those of the profiles across striations. From the currently available data it can therefore be concluded that each deposit has a specific roughness that is possibly inherited from the substrate.

D) There appears to be no systematic difference between the power law exponents of landslides and ejecta. All datasets show the same patterns described above.

References: [1] McSaveney M.J. 1978. In Rockslides and Avalanches 197–258. [2] Naranjo J.A. and Francis P. 1987. Bulletin of Volcanology 49:509–514. [3] McEwen A. 1989. Geology, 17:1111-1114. [4] Lucchitta B.K. 1979. Journal of Geophysical Research 84:8097-8113. [5] Quantin C. et al. 2004. Planetary and Space Science 52:1011–1022. [6] De Blasio F.V. 2011. Planetary and Space Science 59:1384–1392. [7] Watkins J.A. (2015) Geology, 43, 107-110. [8] Boyce J.M. and Mouginis-Mark P.J. 2006. Journal of Geophysical Research 111:E10. [9] Weiss D.K. and Head J.W. (2014) Icarus, 233, 131-146. [10] Wulf G. and Kenkmann T. 2015. Meteoritics and Planetary Science 50:173-203. [11 Shreve R.L. 1966. Science 154, 1639-1643. [12] Barnouin-Jha et al. 2005. Journal of Geophysical Research E: Planets 110, 1–22. [13] Dufresne A. and Davies T.R. 2009. Geomorphology 105:171–181. [14] Moratto Z.M. et al. 2010. 41th Lunar and Planetary Science Conference, Abstract #2364. [15] Malamud B.D. and Turotte D.L. 2001. Journal of Geophysical Research 106, 17,497-17,504.

Additional Information: This work was funded by a stipend of the LGFG of the Albert-Ludwigs Universität Freiburg.